Fundamental modal phenomena on isotropic and anisotropic planar slab dielectric waveguides

Article *in* IEEE Transactions on Antennas and Propagation · May 2003

DOI: 10.1109/TAP.2003.811098 · Source: IEEE Xplore

2 authors:

Alexander B. Yakovlev
University of Mississippi
250 PUBLICATIONS **3,557** CITATIONS
SEE PROFILE

George W. Hanson
University of Wisconsin - Milwaukee
240 PUBLICATIONS **6,862** CITATIONS
SEE PROFILE

Fundamental Modal Phenomena on Isotropic and Anisotropic Planar Slab Dielectric Waveguides

Alexander B. Yakovlev, *Senior Member, IEEE*, and George W. Hanson, *Senior Member, IEEE*

***Abstract*—The characteristic interactions of discrete modes supported by planar isotropic and anisotropic dielectric slab waveguides are analyzed using singularity and critical point theory, leading to a rigorous and complete explanation of all modal interactions. Complex frequency-plane singularities associated with modes on isotropic waveguides are identified and discussed, and the absence of mode coupling is proven. For an anisotropic planar waveguide having an arbitrarily oriented optical axis, it is shown that mode coupling is controlled by the presence of an isolated Morse critical point (MCP) accompanied by a pair of complex-conjugate frequency-plane branch points. The interaction of space-wave leaky modes on a grounded anisotropic slab is studied by investigating the evolution of complex frequency-plane branch point singularities as the orientation of the optical axis varies. The general theory is presented, and numerical results are provided for some specific waveguides.**

***Index Terms*—Anisotropic waveguide, critical points, isotropic waveguide, leaky modes, planar waveguide, singularity theory, waveguide modes.**

I. Introduction

CHARACTERIZATION of modal phenomena on isotropic and anisotropic dielectric waveguides is important in many areas of electromagnetics. In the sinusoidal steady state, knowledge of the dispersion behavior of the discrete and continuous mode spectrum is crucial in the design and analysis of waveguides and waveguide circuits. The exploitation of modal characteristics has lead to a wide array of waveguide-based circuit components, such as couplers, circulators, delay lines, and filters [1]. Furthermore, various mathematical techniques based on mode matching require knowledge of modal dispersion behavior, and modal dispersion underlies the physics of signal dispersion. In the time domain, modal characteristics are exploited in a variety of mathematical modeling techniques for transient wave-layered media interactions [2]–[8].

Dielectric waveguides are often fabricated using isotropic dielectrics, although anisotropic dielectrics may be incorporated either intentionally or unintentionally. Naturally occurring anisotropic materials may be intentionally chosen as a waveguide material for a variety of reasons, such as to enhance polarization-based effects [9]. In addition, waveguide materials may exhibit processing-induced anisotropy, such as often occurs in forming planar layers for circuit boards [10]. Anisotropy can have a significant effect on modal coupling and cutoff properties, and must often be accounted for in electromagnetic simulations for design and analysis of guided-wave structures and devices. In particular, the presence of anisotropy can induce mode coupling in a waveguiding structure that would not admit such coupling when constructed using isotropic materials [11]–[13].

Unfortunately, the dispersion characteristics of all but the simplest waveguiding structures (e.g., homogeneously filled parallel conducting plates or closed rectangular waveguides) must be determined numerically, which obscures the analytical character of the dispersion function. A mathematical model based on the analysis of critical and singular points of the dispersion function can be effectively used for the characterization of the modal spectrum. Of principal interest is the connection of Morse critical points (MCP), fold singular points, and associated frequency-plane branch-point singularities with observable modal phenomena. The role of the MCP in mode-coupling problems has been originally established in [14] and [15] in the analysis of spectral characteristics of open resonators and open waveguides. It has been observed that two solutions in the vicinity of the MCP form a coupling diagram characteristic for a mode-coupling interaction. This idea has been also applied to the analysis of eigenmode coupling in open waveguide resonators [16], [17], metal-dielectric cylindrical waveguides [18], open periodic structures [19], and dielectric layered structures [20], [21].

In recent papers, we have expanded on the investigation of singularities and critical points in printed-circuit transmission lines and dielectric planar slab waveguides. In [22], singular points and associated frequency-plane branch points were shown to govern modal behavior in the vicinity of cutoff in a variety of transmission line and waveguiding structures. In [23], MCPs were shown to provide an alternative to traditional coupled-mode theory for general transmission lines and waveguides. In [24] the TM-even modes supported by an isotropic planar waveguide were studied, and complex frequency-plane branch points associated with these modes were identified. This led to an explanation of the "apparent" modal nonuniqueness of TM-even surface-wave modes supported by a planar waveguide having material loss or gain. In [25] it was shown that branch points are also associated with critical points which occur in mode coupling regions, such that mode interactions will have the form of either mode transformations or mode continuations, depending on the path of frequency variation with respect to the location of the frequency-plane branch points.

In this paper, we 1) extend the results of [24] to include all possible mode classes on isotropic planar waveguides (all

Manuscript received October 15, 2001; revised February 12, 2002.

A. B. Yakovlev is with the Department of Electrical Engineering, The University of Mississippi, University, MS 38677 USA.

G. W. Hanson is with the Department of Electrical Engineering, University of Wisconsin-Milwaukee, Milwaukee, WI 53211 USA.

Digital Object Identifier 10.1109/TAP.2003.811098

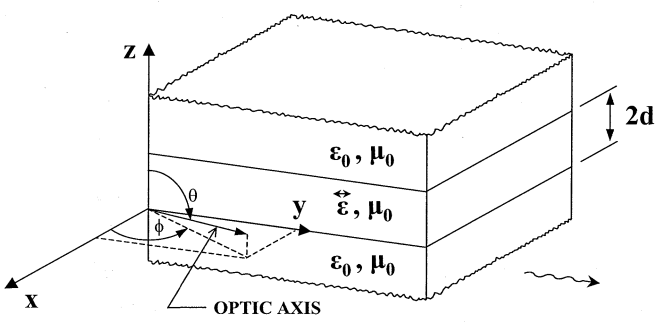

Fig. 1. Planar anisotropic dielectric waveguide.

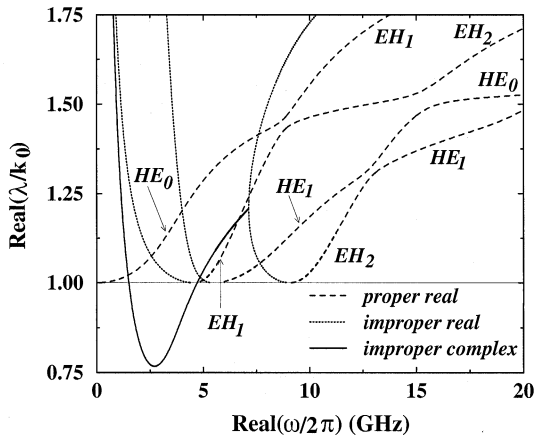

Fig. 2. Dispersion curves for the first four modes of an anisotropic planar waveguide having permittivity (2), where $\varepsilon_{xx} = \varepsilon_{yy} = 4\varepsilon_0$, $\varepsilon_{zz} = 2.25\varepsilon_0$, and $2d = 2$ cm. The optical axis is positioned at $\theta = 45°$ and $\phi = 30°$. The modes are hybrid, and couple together due to the asymmetry provided by the placement of the optical axis.

TM and TE even and odd modes), and discuss the significant differences between the TM and TE mode classes; 2) prove that mode coupling (in the usual sense) cannot occur on isotropic symmetric slab or grounded slab waveguides; 3) prove that modal interactions cannot occur for proper TE modes on isotropic symmetric slab or grounded slab waveguides; and 4) apply the theory of singular and critical points to explain modal phenomena on anisotropic planar dielectric waveguides, making use of the isotropic waveguide results.

Regarding anisotropic waveguides, we present a rigorous theory which explains modal phenomena, in particular modal coupling and transformation, associated with the anisotropic planar waveguide depicted in Fig. 1. For example, typical dispersion curves of several low-order modes for this waveguide are shown in Fig. 2 for the physical parameters $\underline{\underline{\varepsilon}}$ and d provided in the figure caption. Anisotropy-induced modal coupling and transformation between TE^{ρ}-dominant (HE) hybrid modes and TM^{ρ}-dominant (EH) hybrid modes is clearly shown. Because of the hybrid nature of modes on anisotropic waveguides, in order to describe the complex frequency-plane singularities which govern this modal behavior we use the properties obtained for modes on isotropic waveguides.

The paper is organized as follows. In Section II we review the different types of singularities associated with modal phenomena (modal coupling, modal transformation, and modal cutoff). In Section III we discuss singularities associated with discrete modes on an isotropic planar waveguide, treating for the first time TM^{ρ}-odd modes and both types of TE^{ρ} modes. In this section we also prove the absence of coupling among modes, and the absence of modal interaction (in the sense described later) for proper TE modes. Finally, in Section IV we use the results for the isotropic waveguide to explain modal phenomena on anisotropic planar waveguides, including modal coupling and transformation effects associated with proper hybrid surface-wave modes and space-wave leaky modes in the case of a misaligned optical axis.

II. Singularities and Critical Points of the Dispersion Function

Considering the two-dimensional (2-D) planar waveguiding structure depicted in Fig. 1, which is invariant along the waveguiding ρ-axis ($\rho = \sqrt{x^2 + y^2}$), and subsequent to a 2-D Fourier transform in space and time, $(\rho, t) \longleftrightarrow (\lambda, \omega)$, source-free Maxwell's equations and associated boundary conditions can be converted to a functional equation for the discrete modes of the structure

$$A(\lambda, \omega, \underline{\underline{\varepsilon}}, d)X = 0. \tag{1}$$

In (1) λ is the spatial Fourier-transform variable representing the modal propagation constant (note that λ is a radial transform variable, and not wavelength), ω is the temporal Fourier-transform variable representing angular frequency, and X represents a modal field distribution, typically current density, electric field, or magnetic field, depending on the problem formulation. We consider each of the variables (λ, ω) in the complex plane, and assume that $\underline{\underline{\varepsilon}}$ and d have specified values. The dyadic permittivity $\underline{\underline{\varepsilon}}$ is given by

$$\underline{\underline{\varepsilon}} = R^{\intercal}(\theta, \phi) \begin{bmatrix} \varepsilon_{xx} & 0 & 0 \\ 0 & \varepsilon_{yy} & 0 \\ 0 & 0 & \varepsilon_{zz} \end{bmatrix} R(\theta, \phi) \tag{2}$$

where

$$R(\theta, \phi) = \begin{bmatrix} \cos\theta\cos\phi & \cos\theta\sin\phi & -\sin\theta \\ -\sin\phi & \cos\phi & 0 \\ \sin\theta\cos\phi & \sin\theta\sin\phi & \cos\theta \end{bmatrix} \tag{3}$$

represents a rotation matrix which fixes the position of the optical axis, and $R^{\intercal}$ is the transpose of R. Nontrivial solutions of (1) are obtained from the implicit dispersion equation

$$H(\lambda, \omega, \underline{\underline{\varepsilon}}, d) = \det(A(\lambda, \omega, \underline{\underline{\varepsilon}}, d)) = 0. \tag{4}$$

More generally, H is a mapping $(\lambda, \omega, \underline{\underline{\varepsilon}}, d) \to \mathbb{C}$ such that

$$H(\lambda, \omega, \underline{\underline{\varepsilon}}, d) = C \tag{5}$$

where $C \in \mathbb{C}$ is a complex-valued constant, i.e., given $\underline{\underline{\varepsilon}}$ and d only for certain values of (λ, ω) is $C = 0$. By treating (λ, ω) as a pair of complex variables, a study of the properties of the mapping H leads to the analysis of critical points and associated complex frequency-plane branch points which explain modal phenomena. We assume that the mapping H is continuous in (λ, ω), and that all second partial derivatives of H exist and are continuous. For a given formulation this is usually easy to prove.

Since $\underline{\varepsilon}$ and d have specified values, the pair of variables (λ, ω) belongs to one of three possible categories. If

$$\frac{\partial H(\lambda,\omega)}{\partial \lambda} = H'_\lambda(\lambda,\omega) = 0, \quad \frac{\partial H(\lambda,\omega)}{\partial \omega} = H'_\omega(\lambda,\omega) = 0 \tag{6}$$

we call $(\lambda,\omega) = (\lambda_c,\omega_c)$ a *critical point* of the mapping H. If

$$\frac{\partial H(\lambda,\omega)}{\partial \lambda} = H'_\lambda(\lambda,\omega) \neq 0, \quad \frac{\partial H(\lambda,\omega)}{\partial \omega} = H'_\omega(\lambda,\omega) \neq 0 \tag{7}$$

then $(\lambda,\omega) = (\lambda_r,\omega_r)$ is said to be a *regular point* of the mapping H. If

$$\frac{\partial H(\lambda,\omega)}{\partial \lambda} = H'_\lambda(\lambda,\omega) \neq 0, \quad \frac{\partial H(\lambda,\omega)}{\partial \omega} = H'_\omega(\lambda,\omega) = 0 \tag{8}$$

or

$$\frac{\partial H(\lambda,\omega)}{\partial \lambda} = H'_\lambda(\lambda,\omega) = 0, \quad \frac{\partial H(\lambda,\omega)}{\partial \omega} = H'_\omega(\lambda,\omega) \neq 0 \tag{9}$$

then $(\lambda,\omega) = (\lambda_s,\omega_s)$ is said to be a *singular point* of the mapping H.

Furthermore, if

$$H(\lambda,\omega,\underline{\varepsilon},d) = 0 \tag{10}$$

then $(\lambda,\omega) = (\lambda_0,\omega_0)$ is a solution of (4) leading to modal dispersion behavior. In this case we are usually interested in determining the implicit dispersion function $\lambda_0(\omega_0,\underline{\varepsilon},d)$ for the modal propagation constant as a function of frequency. In fact, for any ω_0 one can find a solution λ_0.

Each modal solution point (λ_0, ω_0) of (4) will be either a critical point, a regular point, or a singular point of the mapping H, although, conversely, critical, regular, and singular points of H are not necessarily modal solutions (i.e., they do not necessarily satisfy $H = 0$). From a geometric view, one can consider properties of the surface $[\lambda,\omega,\underline{\varepsilon},d,H(\lambda,\omega,\underline{\varepsilon},d)]$ in the vicinity of the hyperplane $(\lambda,\omega,\underline{\varepsilon},d,0)$.

At a regular or singular point of the mapping H the implicit function theorem states that one can obtain from (4) a unique solution for one of the variables (λ or ω) in terms of the other variable (ω or λ). For example, if $H'_\lambda(\lambda,\omega,\underline{\varepsilon},d) \neq 0$, then (4) admits a unique solution $\lambda(\omega,\underline{\varepsilon},d)$. Furthermore, if H has, for instance, continuous second derivatives, then so does the solution $\lambda(\omega,\underline{\varepsilon},d)$.

In the following sections, we consider critical and singular points of importance in modal interaction problems, both of which lead to branch-point singularities in the complex frequency plane.

A. MCPs

Critical points (λ_c, ω_c) of H may be broadly classified by study of the Hessian

$$\Delta(\lambda_c,\omega_c) = H''_{\lambda\lambda}H''_{\omega\omega} - H''_{\lambda\omega}H''_{\omega\lambda} \tag{11}$$

where all partial derivatives are evaluated at (λ_c, ω_c). For simplicity we assume that $\Delta(\lambda_c,\omega_c)$ is real-valued, which is found to occur for critical points of interest on lossless waveguiding structures. For $\Delta(\lambda_c,\omega_c) < 0$ the critical point represents a saddle point, which occurs in regions of modal coupling [23]. The cases $\Delta(\lambda_c,\omega_c) = 0$ (nonisolated critical point) or $\Delta(\lambda_c,\omega_c) > 0$ (isolated critical point, extremum) are not of interest here.

In particular, we are interested in MCPs $(\lambda_c,\omega_c) = (\lambda_m,\omega_m)$ of the mapping H, which satisfy the set of equations

$$H'_\lambda(\lambda,\omega)\big|_{(\lambda_m,\omega_m)} = 0, \quad H'_\omega(\lambda,\omega)\big|_{(\lambda_m,\omega_m)} = 0, \quad \Delta(\lambda_m,\omega_m) < 0. \tag{12}$$

The Morse lemma [26] shows that H in the vicinity of a MCP can be represented by a quadratic canonical form using a smooth change of variables. The result is the normal form (valid in the vicinity of (λ_m, ω_m)) associated with the MCP

$$(\lambda-\lambda_m)^2 - (\omega-\omega_m)^2 = H(\lambda_m,\omega_m) \tag{13}$$

leading to the dispersion function

$$\lambda(\omega) = \lambda_m \pm \sqrt{H(\lambda_m,\omega_m) + (\omega-\omega_m)^2}. \tag{14}$$

It is obvious that the square root in (14) defines a two-valued function in the complex frequency plane unless $H(\lambda_m,\omega_m) = 0$, i.e., if the Morse point is also a solution of (4). This situation arises in the event of a modal degeneracy.

From (14) the complex frequency-plane branch points $\omega_{b1,2}$ are obtained as complex-conjugate points centered about the real-valued frequency ω_m of the MCP (λ_m, ω_m)

$$\omega_{b1,2} = \omega_m \pm j\sqrt{H(\lambda_m,\omega_m)}. \tag{15}$$

Any frequency contour which passes between the branch points ω_{b1} and ω_{b2} results in mode-coupling in the sense of the usual coupled-mode theory, i.e., mode transformation (hyperbolic-type dispersion) behavior, whereas passing above or below the pair $\omega_{b1,2}$ results in modal interaction with no mode transformation (mode continuation) [25]. At a modal degeneracy given by $H(\lambda_m,\omega_m) = 0$ (of, say, even and odd modes or TM and TE modes, etc.) due to structural symmetry, the branch points $\omega_{b1,2}$ collapse together at the Morse frequency ω_m such that multivalued behavior of the dispersion function in the complex frequency plane vanishes.

It is important to note that MCP theory can also be shown to be locally equivalent to the traditional coupled-mode theory [23], a fact that is key to the proof that modes cannot couple on isotropic slab waveguides, as discussed later.

B. Fold Singular Points

Fold singular points (also known as turning or limit points) (λ_f, ω_f) of the equation $H = 0$ satisfy the set of equations

$$H(\lambda_f,\omega_f) = H'_\lambda(\lambda,\omega)\big|_{(\lambda_f,\omega_f)} = 0, \quad \delta = H''_{\lambda\lambda}(\lambda,\omega)\big|_{(\lambda_f,\omega_f)} H'_\omega(\lambda,\omega)\big|_{(\lambda_f,\omega_f)} \neq 0. \tag{16}$$

The associated normal form (valid in the vicinity of (λ_f, ω_f)) is [27]

$$(\lambda-\lambda_f)^2 + (\omega-\omega_f), \quad \delta > 0, \qquad (\lambda-\lambda_f)^2 - (\omega-\omega_f), \quad \delta < 0 \tag{17}$$

leading to the dispersion function

$$\lambda(\omega) = \lambda_f \pm j\sqrt{\omega-\omega_f}, \quad \delta > 0, \qquad \lambda(\omega) = \lambda_f \pm \sqrt{\omega-\omega_f}, \quad \delta < 0. \tag{18}$$

The square root in (18) clearly implicates frequency-plane branch points at $\omega = \omega_f$, although a more general proof of this using the Weierstrass preparation theorem is provided in [22]. It is found that fold singular points and associated frequency-plane branch points occur in the vicinity of cutoff on a variety of guided-wave structures [22]. In particular, these points correspond to the cutoff points of discrete modes of homogeneously filled parallel plates and, in general, of canonical cylindrical waveguides as resonant eigenvalues of the transverse Laplacian operator defined in the waveguide cross-section. In homogeneously filled cylindrical cavities these points represent resonant frequencies of discrete oscillations. In dielectric waveguides and printed-circuit transmission lines (microstrip, slot line, coplanar waveguide, etc.) fold and branch points describe leaky-wave cutoff behavior. It should also be noted that in a lossless structure fold singular points are real-valued (such that the associated branch points reside on the real frequency axis) separating different modal regimes.

III. Singularities Associated With Isotropic Waveguide Modes

If the structure depicted in Fig. 1 is isotropic, TM^ρ and TE^ρ discrete modes may propagate, governed by the dispersion equations

$$\begin{aligned} H^{\mathrm{TE-odd}}(\lambda,\omega,\varepsilon,d) &= p_1 + p_2\coth(p_2 d) = 0 \\ H^{\mathrm{TE-even}}(\lambda,\omega,\varepsilon,d) &= p_1 + p_2\tanh(p_2 d) = 0 \\ H^{\mathrm{TM-odd}}(\lambda,\omega,\varepsilon,d) &= n_{21}^2 p_1 + p_2\coth(p_2 d) = 0 \\ H^{\mathrm{TM-even}}(\lambda,\omega,\varepsilon,d) &= n_{21}^2 p_1 + p_2\tanh(p_2 d) = 0 \end{aligned} \quad (19)$$

where $p_i = \sqrt{\lambda^2 - k_i^2}$, $\lambda^2 = k_x^2 + k_y^2$, $k_i^2 = n_i^2(\omega/c)^2$, and $c = (\mu_0\varepsilon_0)^{-1/2}$. The isotropic dielectric slab has thickness $2d$, n_2 is the refractive index of the slab, and n_1 corresponds to the semi-infinite dielectrics placed above and below the slab ($n_1 = 1$ for free space), with $n_{21} = n_2/n_1$. The equations for TE-odd and TM-even modes also describe the modes on a grounded slab having thickness d.

The factor p_1 induces branch points in the complex λ-plane at $\lambda = \pm k_1$. Proper (above cutoff) modes reside on the proper Riemann sheet where $\mathrm{Re}(p_1) > 0$, and improper (below cutoff) modes reside on the improper Riemann sheet where $\mathrm{Re}(p_1) < 0$. The branch cuts which separate these two sheets are defined by

$$\mathrm{Re}(p_1) = 0 \quad (20)$$

leading to the standard hyperbolic λ-plane branch cuts

$$\begin{aligned} \mathrm{Im}(\lambda) &= \frac{\mathrm{Im}(k_1)\mathrm{Re}(k_1)}{\mathrm{Re}(\lambda)} \\ |\mathrm{Re}(\lambda)| &< |\mathrm{Re}(k_1)|\,. \end{aligned} \quad (21)$$

The solution of (19) leads to the implicitly defined dispersion function $\lambda_n^{(\pm)}(\omega)$, which provides the dispersion behavior for the nth mode on the proper $(+)$ or improper $(-)$ Riemann sheet. In this paper $n = 0, 2, 4, \ldots$ for even modes and $n = 1, 3, 5, \ldots$ for odd modes. Complex-valued roots are found numerically by a standard secant method root search given a complex-valued initial guess. Once the mode is found at some frequency it is straightforward to "track" the mode as frequency varies. Determining initial guesses requires some trial-and-error, although the propagation constant can usually be found by considering the vicinity of cutoff, where (λ, ω) is approximately known (for TM^ρ modes the vicinity of $(\lambda, 0)$ is also useful).

Since the four equations (19) are independent equations for the four mode classes, it follows that TE^ρ-odd, TE^ρ-even, TM^ρ-odd, and TM^ρ-even modes form mutually independent mode sets, such that no interaction can occur among these mode sets, even in the event of lossy media. However, interactions among modes within a mode set can possibly occur, where we distinguish two possible forms of modal interaction. Mode coupling is when two or more modes exhibit hyperbolic-type dispersion behavior in the sense of the familiar coupled-mode theory. It is shown in [23] that mode coupling is associated with the presence of a nondegenerate MCP pair in the plane (λ, ω), and that coupled-mode theory is locally equivalent to the theory arising from an examination of MCPs. From (12) and using (19) it is easy to prove that a nondegenerate MCP cannot occur (there is no solution of (12) with H given by (19)) for modes on an isotropic slab waveguide. Therefore, mode coupling in the usual sense cannot occur on an isotropic slab (consistent with the fact that mode coupling is usually associated with a perturbation of some "ideal" structure possessing sufficient symmetry, in this case the isotropic slab). More generally, it can be easily shown analytically that in isotropic slabs described by dispersion equations (19), critical points (degenerate, $H = 0$, or nondegenerate, $H \neq 0$) defined by (6) cannot occur. Since MCPs form a subset of critical points, this leads to the conclusion that *in isotropic (single-layer) slabs the dispersion curves of modes within the same set never intersect and they never form hyperbolic-type behavior (mode-coupling)*. The second form of modal interaction (possibly occurring within a mode set) is associated with a mode interchanging with another mode upon encircling (or passing through) a complex-frequency plane branch point, and is discussed later.

A detailed analysis of dispersion behavior and associated complex frequency-plane singularities for the TM^ρ-even modes is given in [24]. For completeness, a summary for the TM^ρ-even modes will be provided here, and the results extended to the other three mode classes, which behave quite differently.

Modal dispersion behavior is shown in Fig. 3 for an isotropic slab having thickness $2d = 2$ cm characterized by $\varepsilon \equiv \varepsilon_2 = 2.25\varepsilon_0$ and $\varepsilon_1 = \varepsilon_0$ when ω varies over the positive real axis. For a given frequency ω, points $(\lambda, \omega) = (\lambda_n^{(\pm)}(\omega), \omega)$ are either regular, singular, or critical points of the mapping $H : (\lambda, \omega, \varepsilon, d) \rightarrow \mathbb{C}$, and are also solutions of (19) if $H(\lambda, \omega, \varepsilon, d) = 0$. As discussed earlier, in the isotropic case critical points, which relate to modal coupling, do not occur. Therefore, all pairs of solution points $(\lambda_n^{(\pm)}(\omega), \omega)$ of (19) shown in Fig. 3 are regular points of the mapping H, except for the singular points (denoted by stars in Fig. 3) where the improper complex solution becomes an improper real solution corresponding to the leaky-wave cutoff.

As described in detail in [24], one can envision modes as occurring in pairs, and certain mode pairs are connected by frequency-plane branch points such that modes in a pair may be

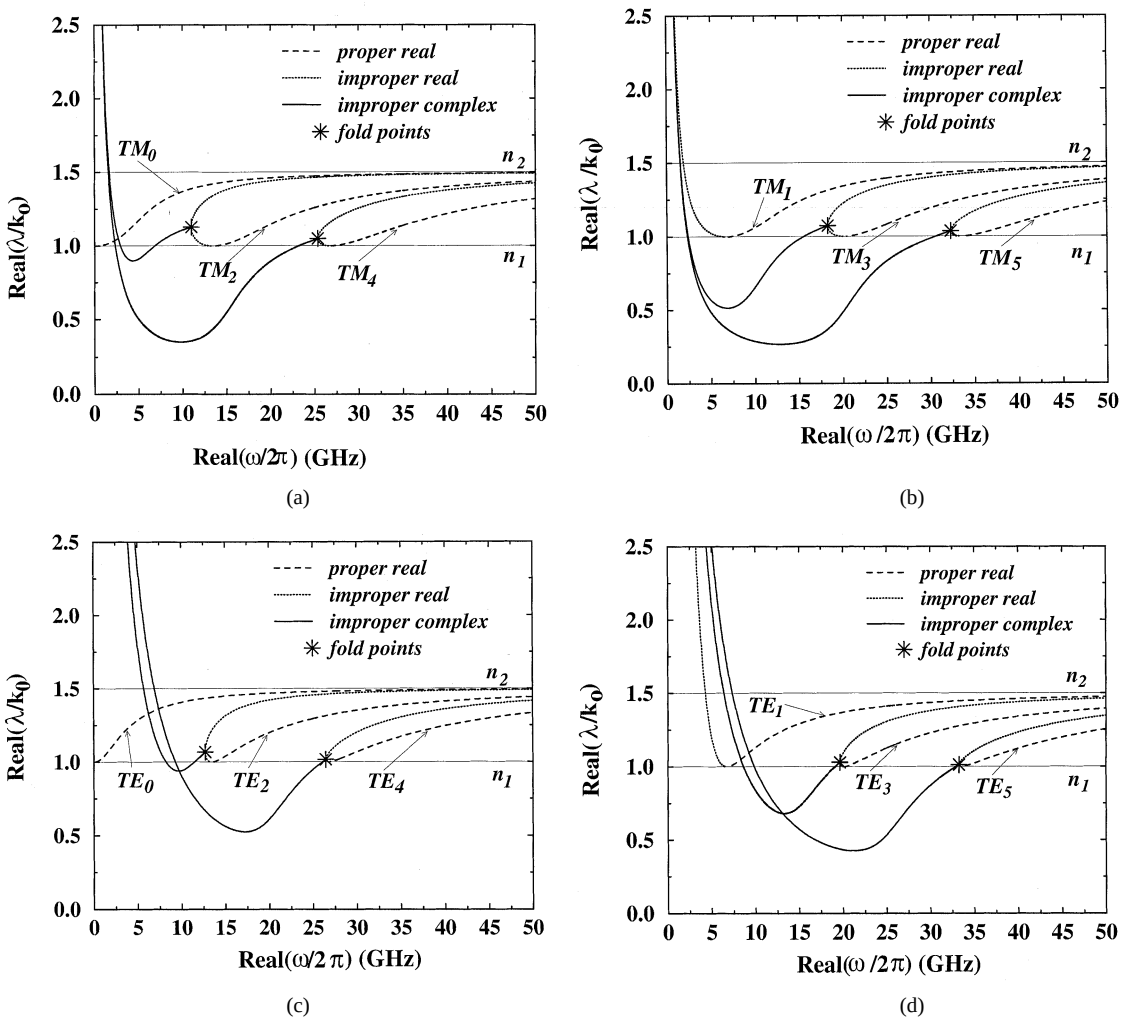

Fig. 3. Dispersion curves of bound and leaky modes for an isotropic planar waveguide having $\varepsilon \equiv \varepsilon_2 = 2.25\varepsilon_0$, $\varepsilon_1 = \varepsilon_0$, and $2d = 2$ cm. (a) TM^ρ-even modes. (b) TM^ρ-odd modes. (c) TE^ρ-even modes. (d) TE^ρ-odd modes. A star symbol denotes the fold singular point associated with the leaky-wave cutoff.

interchanged by encircling the associated branch point. At a frequency-plane branch point of a mode pair, modes in the pair coalesce. Three types of mode pairs have been identified [24], leading to the following characterization.

Modes and their negatives form a Type 0 mode pair $(\lambda_n(\omega), -\lambda_n(\omega))$ such that at a complex frequency $\omega_n^{(0)}$ these modes coalesce, obviously at $\lambda = 0$. These branch points can be determined as

$$\omega_n^{(0)} = \frac{c}{2n_2 d}\left((n-1)\pi \pm j\ln\left(\frac{n_{21}+1}{n_{21}-1}\right)\right) \tag{22}$$

for TM^ρ modes, $n \neq 0$, and

$$\omega_n^{(0)} = \frac{c}{2n_2 d}\left(n\pi \pm j\ln\left(\frac{n_{21}+1}{n_{21}-1}\right)\right) \tag{23}$$

for TE^ρ modes, $n \neq 0$. For the fundamental even TE^ρ and TM^ρ modes having $n = 0$, $\omega_0^{(0)} = 0$. These points are first-order branch points for a mode pair consisting of a mode and its negative.

Modes and their conjugates form a Type 1 mode pair $(\lambda_n(\omega), \overline{\lambda}_n(\omega))$ such that at a frequency $\omega_n^{(1)}$ these modes coalesce, obviously on the real-ω axis. A complete revolution about $\omega_n^{(1)}$ results in the smooth interchange of a mode and its conjugate, such that $\omega_n^{(1)}$ are first-order branch points for the nth mode and its conjugate. The $\omega_n^{(1)}$ branch points are located on the real-ω axis for lossless media, near to and at a value less than the well-known cutoff frequency points of discrete modes

$$\omega_n^c = \frac{n\pi c}{2d\sqrt{n_2^2 - n_1^2}} \tag{24}$$

and can be found numerically from (16). In isotropic dielectric slabs the $\omega_n^{(1)}$ branch points correspond to the leaky-wave cutoff frequency points.

A given mode $\lambda_n(\omega)$ and the next higher-order mode with the same symmetry (even or odd) about the plane $z = d$ (Fig. 1), $-\lambda_{n+2}(\omega)$, form a Type 2 mode pair. At a frequency $\omega_{n/n+2}^{(2)}$ modes in the pair coalesce, and a complete rotation about $\omega_{n/n+2}^{(2)}$ results in the smooth interchange of the $\pm nth$ and $\mp(n+2)th$ modes. As such, $\omega_{n/n+2}^{(2)}$ are first-order branch points for the nth and $-(n+2)th$ modes. These branch points can also be found numerically from (16). It is easy to show that TE^ρ proper modes do not possess Type 2 branch points: for TE^ρ modes with $\lambda \neq 0$, (16) leads to $p_1 d = -1$. However, for

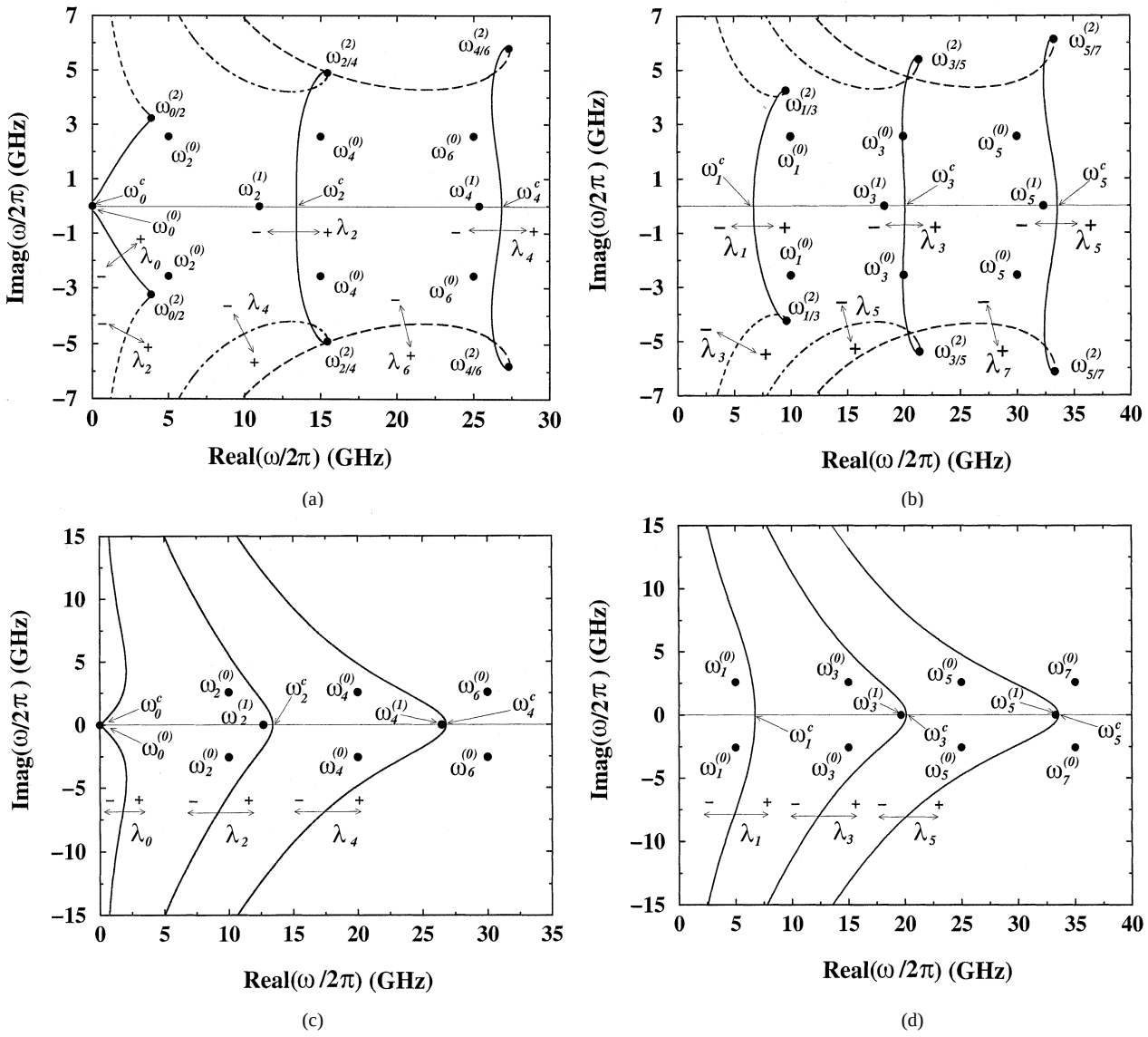

Fig. 4. Complex frequency-plane singularities (dots) of different types, generalized cutoff-frequency loci (solid and dashed lines), and ordinary cutoff frequencies for the modes of an isotropic planar waveguide having $\varepsilon \equiv \varepsilon_2 = 2.25\varepsilon_0$, $\varepsilon_1 = \varepsilon_0$, and $2d = 2$ cm. (a) TM^ρ-even modes. (b) TM^ρ-odd modes. (c) TE^ρ-even modes. (d) TE^ρ-odd modes. Type 2 branch points $\omega^{(2)}_{n/n+2}$ do not occur for TE^ρ modes (cases (c) and (d)).

proper modes $\mathrm{Re}(p_1) > 0$. Therefore, Type 2 branch points cannot exist for TE^ρ proper modes, and the complicated modal interaction possible for TM modes, especially for lossy media, cannot occur. From duality, if magnetic contrast is included this statement no longer holds.

All of these branch points are shown in Fig. 4 for the four different mode classes. Note that the complex frequency plane is simpler for the TE^ρ modes compared to the TM^ρ modes, due to the absence of Type 2 branch points for TE^ρ modes. Also shown in Fig. 4 are the cutoff frequencies ω^c_n, as well as the generalized cutoff frequencies given by the solid and dashed lines. As discussed in [24], the locus of complex frequencies for which a mode crosses the λ-plane branch cuts are called generalized cutoff frequencies, and in the case of real ω this reduces to the usual definition of cutoff frequency. These generalized cutoff frequencies will satisfy (1), along with the additional condition $\mathrm{Re}(p_1) = 0$. Unfortunately, this does not lead to an explicit formula for the locus of generalized cutoff frequencies, but rather yields three real equations in three real unknowns (ω_r, ω_i, and λ_r or λ_i). The generalized cutoff frequencies extend the concept of modal cutoff to the case of complex ω and lossy media, and are described more thoroughly in [24].

Although many of the above described branch points occur in the complex frequency plane away from the real axis, if they are located on or near to the real-ω axis they will significantly influence time-harmonic dispersion behavior. For instance, when material loss or gain is present, the $\omega^{(0)}_n$ and $\omega^{(2)}_{n/n+2}$ branch points may migrate across the real-ω axis, causing modal interchange and apparent modal nonuniqueness [24]. The $\omega^{(1)}_n$ branch points leave the real-ω axis in the event of material loss or gain, explaining dispersion behavior in the "spectral-gap" region in these cases. Apart from time-harmonic wave phenomena, if the various branch points migrate in the complex ω-plane due to changes in the material or geometric properties of the waveguide, transient methods such as [8] which use modal properties are significantly affected.

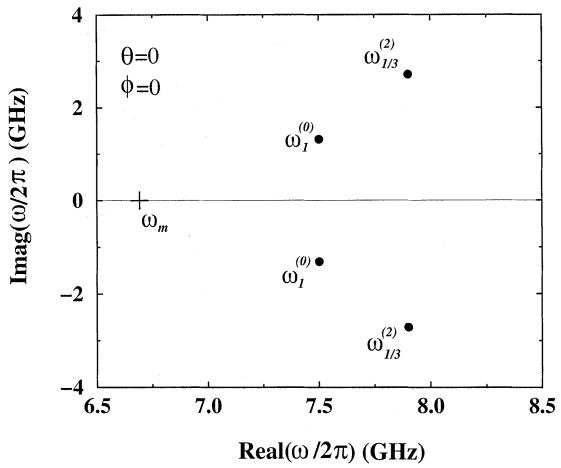

(a)

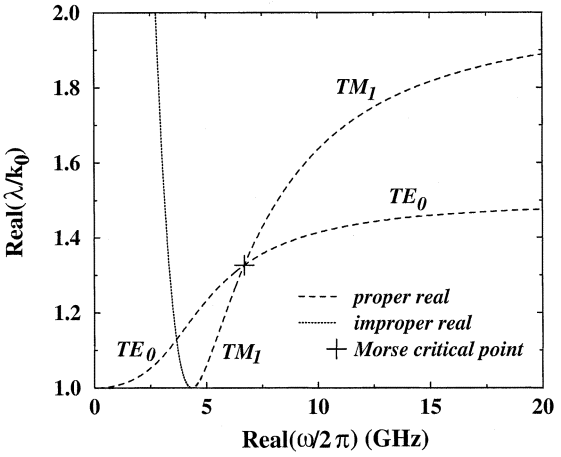

(b)

Fig. 5. (a) Complex frequency-plane singularities associated with the first two modes shown in Fig. 2. The optical axis is positioned at $\theta = 0^\circ$ (pure uncoupled TE^ρ and TM^ρ modes exist). (b) Dispersion curves for the first two modes shown in Fig. 2 when the optical axis is positioned at $\theta = 0^\circ$. The location of a degenerate MCP given by (12) is shown by the plus sign at the place of intersection of dispersion curves.

IV. Singularities Associated With Anisotropic Waveguide Modes

If the planar waveguide depicted in Fig. 1 is anisotropic, the dispersion equation (4) which governs modal phenomena becomes more complicated than (19). For this work the dispersion equation (4) was obtained numerically using the method described in [28]. In Fig. 2 dispersion curves for the first four modes of an anisotropic planar waveguide having permittivity (2) are shown, where $\varepsilon_{xx} = \varepsilon_{yy} = 4\varepsilon_0$, $\varepsilon_{zz} = 2.25\varepsilon_0$, and $2d = 2$ cm. The optical axis is positioned at $\theta = 45^\circ$ and $\phi = 30^\circ$ such that the modes are hybrid, and couple together due to the asymmetry provided by the placement of the optical axis [13] (this asymmetry forms the required perturbation of the "ideal" (isotropic) structure to result in mode coupling).

In order to understand the reason for modal coupling, consider hybrid discrete modes EH_1 and HE_0. These modes are associated with the TM_1 and TE_0 modes on an isotropic waveguide having $\varepsilon_{xx} = \varepsilon_{yy} = \varepsilon_{zz} = 2.25\varepsilon_0$. The various ω-plane singularities associated with the TM_1 and TE_0 modes (and some others) are shown in Fig. 4(b) and (c), respectively. Starting with the isotropic case, if ε_{zz} is fixed at $2.25\varepsilon_0$ and $\varepsilon_{xx} = \varepsilon_{yy}$ is increased from $2.25\varepsilon_0$ to $4\varepsilon_0$, the waveguide material obviously becomes anisotropic with $\theta = 0^\circ$. The branch point singularities associated with the isotropic modes shown in Fig. 4(b) and (c) migrate (somewhat uneventfully) in the complex ω-plane, to become located as shown in Fig. 5(a). An important new feature is that a MCP ω_m appears for the anisotropic case. For the isotropic case the MCP does not exist as discussed previously (it can be thought of as being located at infinity), and as the material becomes anisotropic the point ω_m moves in from infinity (toward the origin) along the real-ω axis. For $\theta = 0^\circ$ this critical point is degenerate, in the sense that $H(\lambda_m, \omega_m) = 0$, and in this case the dispersion curves given by (14) form (locally) two intersecting straight lines, indicating that the modes do not couple (pure TE^ρ and TM^ρ modes exist). This is shown in Fig. 5(b).

As the optical axis is moved away from a coordinate axis the modes generally become hybrid (although pure TE and TM modes do still exist if the optical axis is moved in certain planes). Some of the branch points in Fig. 5(a) migrate as well, although the most important effect is that the MCP becomes nondegenerate, in the sense that $H(\lambda_m, \omega_m) \neq 0$, leading to associated branch-point singularities given by (15). The location of the various singularities associated with these first two modes are shown in Fig. 6(a) for the optical axis positioned at $\theta = 45^\circ$ and $\phi = 30^\circ$ (the case of $\theta = 60^\circ$ and $\phi = 30^\circ$ is also shown in this figure). The branch points $\omega_{b1,2}$ given by (15) are denoted by $\omega_{0/1}^{(m1,2)}$ in the figure, since they connect the $n = 0$ TE-even mode and the $n = 1$ TM-odd mode. These branch points split apart from the MCP ω_m as the optical axis moves from $\theta = 0^\circ$, and reside symmetrically about the real-ω axis for $\theta \neq 0, \pi$. Since the path of frequency variation passes between these points, mode coupling and associated mode transformation occurs [25]. In this case the dispersion curves for these modes are shown in Fig. 6(b) (also shown in Fig. 2).

The migration of the MCP and branch points, as well as the splitting off of the branch points $\omega_{0/1}^{(m1,2)}$ from the MCP as the pure TE and TM modes become hybrid, is shown in Fig. 7. The solid lines show migration of the branch points for $\varepsilon_{zz} = 2.25\varepsilon_0$ as $\varepsilon_{xx} = \varepsilon_{yy}$ changes from $2.25\varepsilon_0$ (isotropic case, shown in Fig. 4) to $\varepsilon_{xx} = \varepsilon_{yy} = 4\varepsilon_0$ (anisotropic case). The dashed lines show the migration as θ is then changed from 0° to 60° in the plane $\phi = 30^\circ$. As the material becomes anisotropic the MCP moves from infinity to the finite ω-plane (in Fig. 7, $\omega_m/2\pi = 6.6921$ GHz for $\varepsilon_{xx} = \varepsilon_{yy} = 4\varepsilon_0$ and $\varepsilon_{zz} = 2.25\varepsilon_0$), and as θ moves away from 0, ω_m migrates as shown (at $\theta = 45^\circ$, $\omega_m/2\pi = 8.904$ GHz and at $\theta = 60^\circ$, $\omega_m/2\pi = 10.179$ GHz) and branch points $\omega_{0/1}^{(m1,2)}$ associated with the nondegenerate MCP emerge (these branch points coalesce at the MCP if θ is brought back to 0).

Finally, as another application we consider the migration of $\omega_{n/n+2}^{(2)}$ branch points which cause leaky modes to interact (similarly, for the case of an isotropic slab, varying material loss causes the $\omega_{n/n+2}^{(2)}$ points to migrate across the real-ω axis, causing proper modes to interact, as described in [24]). We consider a grounded anisotropic slab having $d = 1$ cm,

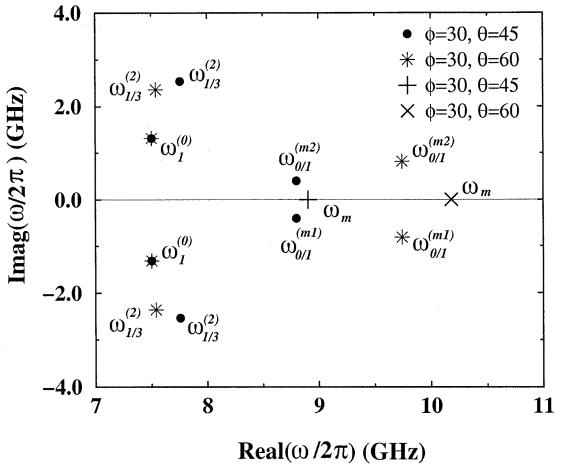

(a)

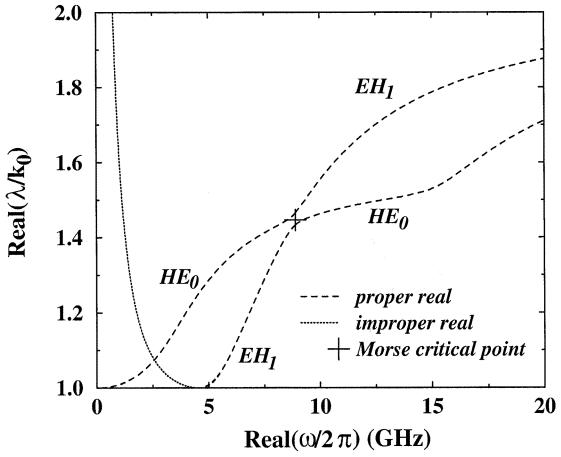

(b)

Fig. 6. (a) Complex frequency-plane singularities associated with the first two modes shown in Fig. 2. The optical axis is positioned at $\theta = 45^\circ$ and $\phi = 30^\circ$ (coupled hybrid HE^{ρ} and EH^{ρ} modes exist). Note the presence of the branch points $\omega_{n/m}^{(m1,2)}$ given by (15) and associated with the nondegenerate MCP. The case of $\theta = 60^\circ$ and $\phi = 30^\circ$ is also shown to demonstrate the evolution of singularities. (b) Dispersion curves for the first two modes shown in Fig. 2 when the optical axis is positioned at $\theta = 45^\circ$ and $\phi = 30^\circ$. The location of the nondegenerate MCP given by (12) is shown by the plus sign in the region of mode transformation.

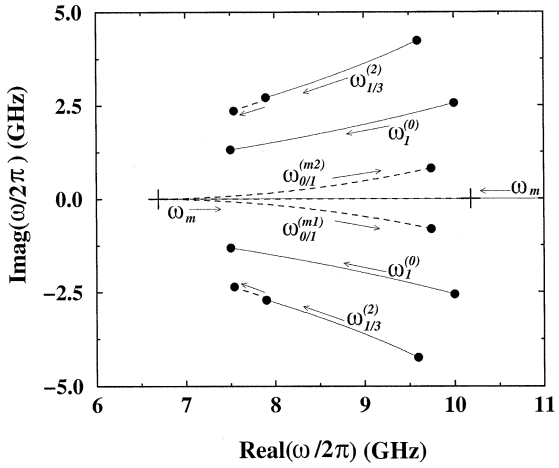

Fig. 7. Migration (parameterized) in the complex frequency plane of various branch points and the MCP associated with the first two modes shown in Fig. 2. The solid lines represent migration of the branch points for $\varepsilon_{zz} = 2.25\varepsilon_0$ as $\varepsilon_{xx} = \varepsilon_{yy}$ changes from $2.25\varepsilon_0$ (isotropic case shown in Fig. 4) to $\varepsilon_{xx} = \varepsilon_{yy} = 4\varepsilon_0$ (anisotropic case). The dashed lines show the migration of these points as θ is changed from 0° to 60° in the plane $\phi = 30^\circ$. As the material becomes anisotropic the MCP moves from infinity to the finite ω-plane, and as θ varies and the modes become hybrid, ω_m migrates as shown and branch points $\omega_{0/1}^{(m1,2)}$ associated with the nondegenerate MCP emerge (these branch points coalesce at the MCP when $\theta = 0^\circ$ and the modes decouple).

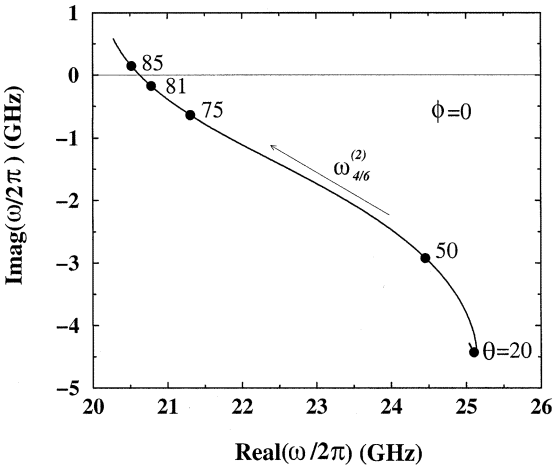

Fig. 8. Migration of complex frequency-plane branch point $\omega_{4/6}^{(2)}$ parameterized by θ for a grounded anisotropic slab aveguide having $d = 1$ cm, $\varepsilon_{xx} = \varepsilon_{yy} = 2.25\varepsilon_0$, and $\varepsilon_{zz} = 4\varepsilon_0$. As θ varies the branch point migrates across the real-frequency axis separating two different modal interaction regimes. The branch point crosses the real-frequency axis at approximately $\theta = 83^\circ$ resulting in degeneracy of the leaky modes EH_4 and EH_6.

$\varepsilon_{xx} = \varepsilon_{yy} = 2.25\varepsilon_0$, and $\varepsilon_{zz} = 4\varepsilon_0$. As θ varies in the xz-plane ($\phi = 0$) the point $\omega_{4/6}^{(2)}$ migrates toward the real-ω axis, and crosses the axis at approximately $\theta = 83^\circ$ as shown in Fig. 8. The corresponding dispersion behavior is shown in Fig. 9 for $\theta = 81^\circ$ (just before the branch point crosses the real-ω axis, $\omega_{4/6}^{(2)} = 20.7854 - j0.1771$ GHz), and in Fig. 10 for $\theta = 85^\circ$ (just after the branch point crosses the real-ω axis, $\omega_{4/6}^{(2)} = 20.5194 + j0.1542$ GHz). In Fig. 9, where the frequency path is above the branch point $\omega_{4/6}^{(2)}$, EH_4 and EH_6 leaky modes interact but do not interchange (EH_4 and EH_6 leaky modes eventually become EH_4 and EH_6 proper (surface-wave) modes, respectively). In Fig. 10 the frequency path is below the branch point $\omega_{4/6}^{(2)}$. In this case the leaky mode EH_4 (EH_6) analytically continues to become the leaky mode EH_6 (EH_4) associated with the proper mode EH_6 (EH_4). These figures show that even for lossless media modal interactions, leading to what would otherwise be interpreted as mode nonuniqueness, can be explained by an understanding of complex frequency-plane branch points associated with mode pairs, and their associated migrations as material or geometrical parameters vary.

V. Conclusion

In this paper we have used the theory of critical and singular points in the complex frequency plane to explain modal phenomena on planar dielectric waveguides. The theory was first applied to an isotropic dielectric waveguide, where a variety of complex plane features were examined. As the isotropic

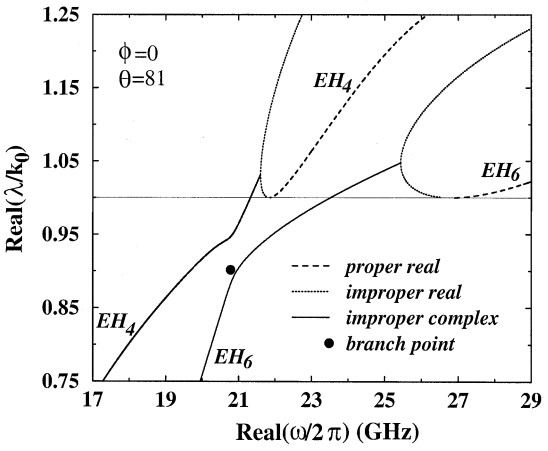

(a)

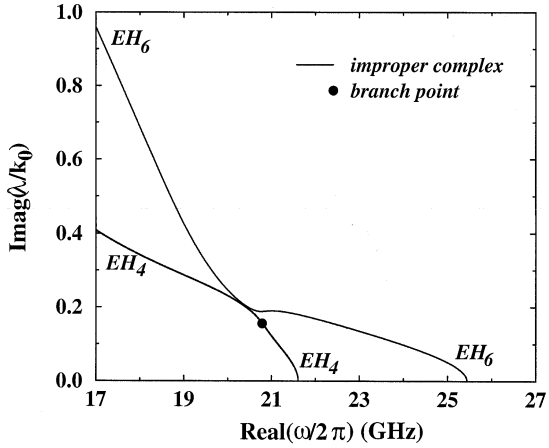

(b)

Fig. 9. Dispersion curves [(a) phase constant and (b) attenuation constant] for the leaky modes EH_4 and EH_6 on a grounded anisotropic slab when the optical axis is positioned at $\theta = 81^\circ$, $\phi = 0^\circ$. The branch point $\omega_{4/6}^{(2)}$ is close to and below the real-frequency axis (frequency path). In this case the leaky modes EH_4 and EH_6 interact but do not interchange.

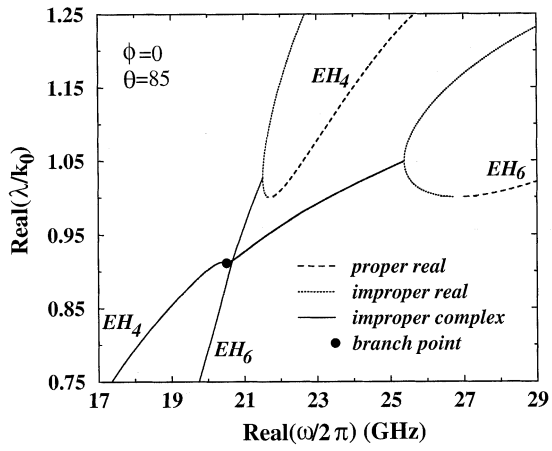

(a)

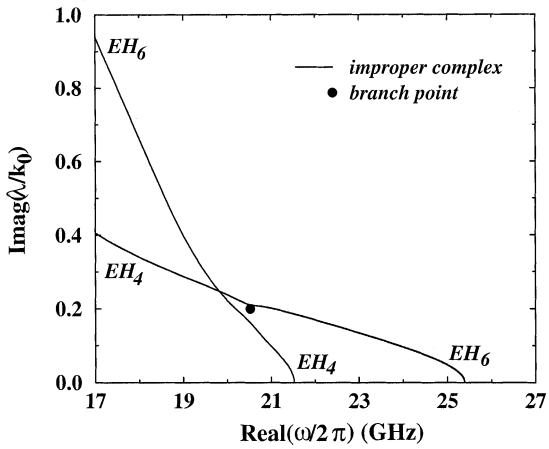

(b)

Fig. 10. Dispersion curves [(a) phase constant and (b) attenuation constant] for the leaky modes EH_4 and EH_6 when the optical axis is positioned at $\theta = 85^\circ$, $\phi = 0^\circ$. The branch point $\omega_{4/6}^{(2)}$ is close to and above the real-frequency axis corresponding to the analytical continuation of mode EH_4 (EH_6) to mode EH_6 (EH_4).

material in the waveguide was transformed into an anisotropic medium, it was shown that the singularities and critical points associated with the isotropic waveguide migrate in the complex frequency plane. This migration was used to explain modal coupling, modal transformation, and modal interaction phenomena of discrete hybrid surface waves and space-wave leaky modes for the case of an anisotropic slab waveguide.

REFERENCES

[1] B. L. Smith and M. H. Carpentier, *The Microwave Engineering Handbook*. New York: Van Nostrand Reinhold, 1993.

[2] L. Tsang and J. A. Kong, "Modified modal theory of transient response in layered media," *J. Math Phys*, vol. 20, no. 6, pp. 1170–1182, June 1979.

[3] A. Ezzeddine, J. A. Kong, and L. Tsang, "Time response of a vertical electric dipole over a two-layer medium by the double deformation technique," *J. Appl. Phys*, vol. 53, no. 2, pp. 813–822, Feb. 1982.

[4] L. B. Felsen and F. Niu, "Spectral analysis and synthesis options for short pulse radiation from a point dipole in a grounded dielectric layer," *IEEE Trans. Antennas Propagat.*, vol. 41, pp. 747–754, June 1993.

[5] F. Niu and L. B. Felsen, "Time-domain leaky modes on layered media: dispersion characteristics and synthesis of pulsed radiation," *IEEE Trans. Antennas Propagat.*, vol. 41, pp. 755–761, June 1993.

[6] ——, "Asymptotic analysis and numerical evaluation of short pulse radiation from a point dipole in a grounded dielectric layer," *IEEE Trans. Antennas Propagat.*, vol. 41, pp. 762–769, June 1993.

[7] R. A. W. Haddon, "Exact evaluation of the response of a layered elastic medium to an explosive point source using leaking modes," *Bull. Seism. Soc. Amer.*, vol. 76, no. 6, pp. 1755–1775, Dec. 1986.

[8] G. W. Hanson, A. B. Yakovlev, and J. Hao, "Leaky-wave analysis of transient fields due to sources in planarly-layered media," *IEEE Trans. Antennas Propagat.*, vol. 51, pp. 146–159, Feb., 2003.

[9] K. Kitayama and N. Kumagai, "Theory and applications of coupled optical waveguides involving anisotropic or gyrotropic materials," *IEEE Trans. Microwave Theory Tech.*, vol. MTT-25, pp. 567–572, July 1977.

[10] N. G. Alexopoulus, "Integrated-circuit structures on anisotropic substrates," *IEEE Trans. Microwave Theory Tech.*, vol. MTT-33, pp. 847–881, Oct. 1985.

[11] D. Marcuse and I. P. Kaminow, "Modes of a symmetric slab optical waveguide in birefringent media, part II: slab with coplanar optical axis," *IEEE J. Quantum Electron.*, vol. QE-15, pp. 92–101, Feb. 1979.

[12] L. Torner, J. Recolons, and J. P. Torres, "Guided-to-leaky mode transformation in uniaxial optical slab waveguides," *J. Lightwave Technol.*, vol. 11, pp. 1592–1600, Oct. 1993.

[13] A. Knoesen, T. K. Gaylord, and M. G. Moharam, "Hybrid guided modes in uniaxial dielectric planar waveguides," *J. Lightwave Technol.*, pp. 1083–1103, June 1988.

[14] P. N. Melezhik, A. Y. Poyedinchuk, Y. A. Tuchkin, and V. P. Shestopalov, "Properties of spectral characteristics of the open two-mirror resonator," *Dokl. Akad. Nauk URSR*, ser. A, no. 8, pp. 51–54, 1987.

[15] ——, "Analytical nature of the vibrational mode-coupling phenomenon," *Dokl. Akad. Nauk SSSR*, vol. 300, no. 6, pp. 1356–1359, 1988.
[16] V. P. Shestopalov, "Morse critical points of dispersion equations of open resonators," *Electromagnetics*, vol. 13, pp. 239–253, 1993.
[17] I. E. Pochanina and N. P. Yashina, "Electromagnetic properties of open waveguide resonators," *Electromagnetics*, vol. 13, pp. 289–300, 1993.
[18] A. Svezhentsev, "Special points of dispersion equations of metal-dielectric cylindrical waveguides," *Dokl. Akad. Nauk URSR*, no. 4, pp. 82–87, 1994.
[19] V. P. Shestopalov and V. V. Yatsik, "Morse critical points of grating free oscillations and waves," *Radiophys. Quantum Electron.*, vol. 36, no. 9, pp. 623–629, 1993.
[20] ——, "Spectral theory of a dielectric layer and the Morse critical points of dispersion equations," *Ukrainian J. Phys.*, vol. 42, no. 7, pp. 861–869, 1997.
[21] ——, "Morse critical points of the dispersion equations and evolution equations of a quasi homogeneous structure," *Ukrainian J. Phys.*, vol. 45, no. 6, pp. 744–752, 2000.
[22] G. W. Hanson and A. B. Yakovlev, "An analysis of leaky-wave dispersion phenomena in the vicinity of cutoff using complex frequency plane singularities," *Radio Science*, vol. 33, no. 4, pp. 803–820, July–Aug. 1998.
[23] A. B. Yakovlev and G. W. Hanson, "Analysis of mode coupling on guided-wave structures using Morse critical points," *IEEE Trans. Microwave Theory Tech.*, vol. 46, pp. 966–974, July 1998.
[24] G. W. Hanson and A. B. Yakovlev, "Investigation of mode interaction on planar dielectric waveguides with loss and gain," *Radio Science*, vol. 34, no. 6, pp. 1349–1359, Nov.–Dec. 1999.
[25] A. B. Yakovlev and G. W. Hanson, "Mode-transformation and mode-continuation regimes on waveguiding structures," *IEEE Trans. Microwave Theory Tech.*, vol. 48, pp. 67–75, Jan. 2000.
[26] T. Poston and I. Stewart, *Catastrophe Theory and Its Applications*: Dover, 1978.
[27] M. Golubitsky and D. G. Schaeffer, *Singularities and Groups in Bifurcation Theory*. Berlin: Springer-Verlag, 1985, vol. 1.
[28] G. W. Hanson, "A numerical formulation of dyadic Green's functions for planar bianisotropic media with application to printed transmission lines," *IEEE Trans. Microwave Theory Tech.*, vol. 44, pp. 144–151, Jan. 1996.

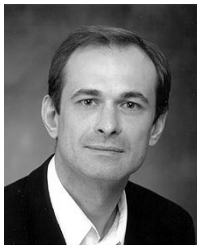

Alexander B. Yakovlev (S'94–M'97–SM'01) was born on June 5, 1964, in the Ukraine. He received the Ph.D. degree in radiophysics from the Institute of Radiophysics and Electronics, National Academy of Sciences, Ukraine, in 1992, and the Ph.D. degree in electrical engineering from the University of Wisconsin at Milwaukee, in 1997.

From 1992 to 1994, he was an Assistant Professor with the Department of Radiophysics, Dnepropetrovsk State University, Ukraine. From 1994 to 1997, he was a Research and Teaching Assistant with the Department of Electrical Engineering and Computer Science, University of Wisconsin at Milwaukee. From 1997 to 1998, he was an R&D Engineer in Ansoft Corporation/Compact Software Division, Paterson, NJ, and in Ansoft Corporation, Pittsburgh, PA. From 1998 to 2000, he was a Postdoctoral Research Associate with the Electrical and Computer Engineering Department at North Carolina State University, Raleigh, NC. In summer 2000, he joined the Department of Electrical Engineering, The University of Mississippi, University, as an Assistant Professor. His research interests include mathematical methods in applied electromagnetics, modeling of high-frequency interconnection structures and amplifier arrays for spatial and quasioptical power combining, integrated-circuit elements and devices, theory of leaky waves, and singularity theory.

Dr. Yakovlev received the Young Scientist Award presented at the 1992 URSI International Symposium on Electromagnetic Theory, Sydney, Australia, and the Young Scientist Award at the 1996 International Symposium on Antennas and Propagation, Chiba, Japan. He is a member of URSI Commission B.

George W. Hanson (S'85–M'91–SM'98) was born in Glen Ridge, NJ, in 1963. He received the B.S.E.E. degree from Lehigh University, Bethlehem, PA, the M.S.E.E. degree from Southern Methodist University, Dallas, TX, and the Ph.D. degree from Michigan State University, East Lansing, in 1986, 1988, and 1991, respectively.

From 1986 to 1988, he was a development engineer with General Dynamics in Fort Worth, TX, where he worked on radar simulators. From 1988 to 1991, he was a research and teaching assistant with the Department of Electrical Engineering, Michigan State University. He is currently an Associate Professor of electrical engineering and computer science at the University of Wisconsin in Milwaukee. His research interests include electromagnetic wave phenomena in layered media and microwave characterization of materials.

Dr. Hanson is a member of URSI Commission B, Sigma Xi, and Eta Kappa Nu.